Function of MoaB Proteins in the Biosynthesis of the Molybdenum and Tungsten Cofactors†

Loes E. Bevers,‡,§ Peter-Leon Hagedoorn,‡ José A. Santamaria-Araujo,§ Axel Magalon,|| Wilfred R. Hagen,‡ and Guenter Schwarz*,§

Department of Biotechnology, Delft University of Technology, Delft, the Netherlands, Institute of Biochemistry, University of Cologne, 50674 Cologne, Germany, and Laboratoire de Chimie Bactérienne, Institut de Biologie Structurale et Microbiologie, Centre National de la Recherche Scientifique, Marseille, France

Received October 11, 2007; Revised Manuscript Received November 13, 2007

ABSTRACT: Molybdenum (Mo) and tungsten (W) enzymes catalyze important redox reactions in the global carbon, nitrogen, and sulfur cycles. Except in nitrogenases both metals are exclusively associated with a unique metal-binding pterin (MPT) that is synthesized by a conserved multistep biosynthetic pathway, which ends with the insertion and thereby biological activation of the respective element. Although the biosynthesis of Mo cofactors has been intensively studied in various systems, the biogenesis of W-containing enzymes, mostly found in archaea, is poorly understood. Here, we describe the function of the *Pyrococcus furiosus* MoaB protein that is homologous to bacterial (such as MogA) and eukaryotic proteins (such as Cnx1) involved in the final steps of Mo cofactor synthesis. MoaB reconstituted the function of the homologous *Escherichia coli* MogA protein and catalyzes the adenylylation of MPT in a Mg^{2+} and ATP-dependent way. At room temperature reaction velocity was similar to that of the previously described plant Cnx1G domain, but it was increased up to 20-fold at 80 °C. Metal and nucleotide specificity for MPT adenylylation is well conserved between W and Mo cofactor synthesis. Thermostability of MoaB is believed to rely on its hexameric structure, whereas homologous mesophilic MogA-related proteins form trimers. Comparison of *P. furiosus* MoaB to *E. coli* MoaB and MogA revealed that only MogA is able to catalyze MPT adenylylation, whereas *E. coli* MoaB is inactive. In summary, MogA, Cnx1G, and MoaB proteins exhibit the same adenylyl transfer activity essential for metal insertion in W or Mo cofactor maturation.

Tungsten and molybdenum are transition metals with very similar properties. They both have an essential role in biology as they are present in cofactors of enzymes that mainly catalyze oxygen atom transfer reactions. Mo enzymes are ubiquitous in all forms of life (*1*), whereas W-containing enzymes have only been identified in prokaryotes (predominantly archaea) so far (*2*). Both metals are bound to the same type of cofactor, which consists of one or two tricyclic pyranopterin moieties originally described as molybdopterin (*3*) but now called metal-binding pterin (MPT[1]) (*4*). The metals are coordinated by the dithiolene sulfurs in the pyranoring of MPT. In the case of tungsten, there are always two pterin moieties present resulting in the four sulfur-coordinated tungsten bispterin cofactor (Wco) (*5*).

Mo cofactor (Moco)-containing enzymes can be classified into three separate families based on the coordination of the molybdenum (*6*). Dimethyl sulfoxide oxidoreductases (DMSORs) contain a bispterin cofactor modified by nucleotide monophosphates covalently attached to the terminal phosphate of each MPT molecule. The DMSOR-type cofactors of Mo enzymes are directly related to one of the two families of Wco-containing enzymes, which comprises formate dehydrogenases (FDHs) found in *Pyrococcus furiosus* (*7*) and other archaea. The other class of Wco-dependent enzymes comprises unique enzymes that form the family of W-containing aldehyde oxidoreductases. Five of these enzymes have been identified from the hyperthermophilic archaeon *P. furiosus*: aldehyde oxidoreductase (*8*), formaldehyde oxidoreductase (*9*), glyceraldehyde-3-phosphate oxidoreductase (*10*), tungsten-containing oxidoreductase 4 (*11*), and tungsten-containing oxidoreductase 5 (*12*) that all share a bispterin Wco without nucleotide modification.

The biosynthetic pathway of MPT cofactors has been extensively studied for Moco in bacteria as well as in higher eukaryotes and appears to be highly conserved (*4*). In brief, GTP is converted in an *S*-adenosyl methionine-dependent reaction to cyclic pyranopterin monophosphate. In the second step two sulfur atoms are transferred by the heterotetrameric MPT synthase, which consists of two large and two small subunits. Only recently, details on the third, metal insertion,

† This work was supported by grants from the Council for Chemical Sciences of the Netherlands Organization for Scientific Research (700.51.301 to W.R.H.), the Deutsche Forschungsgemeinschaft (G.S.), the Bundesministerium für Bildung und Forschung (G.S.), and Fonds der Chemischen Industrie (G.S.).

* To whom correspondence should be addressed. Tel.: +49-221-470 6432. Fax: + 49-221-470 6731. E-mail: gschwarz@uni-koeln.de.

‡ Delft University of Technology.

§ University of Cologne.

|| Centre National de la Recherche Scientifique.

[1] Abbreviations: DMSOR, dimethyl sulfoxide reductase; EcMoaB, *E. coli* MoaB; EcMogA, *E. coli* MogA; FDH, formate dehydrogenase; Moco, molybdenum cofactor; MPT, molybdopterin; PfMoaB, *P. furiosus* MoaB; Wco, tungsten cofactor; cPMP, cyclic pyranopterin monophosphate.

10.1021/bi7020487 CCC: $40.75
Published on Web 12/22/2007

step have been obtained by the characterization of plant Cnx1 protein that combines functions of two homologous bacterial proteins (MoeA and MogA) in a single two-domain protein (E and G). Cnx1G binds MPT with high affinity (*13*) and catalyzes an adenylyl transfer to the MPT phosphate yielding MPT−AMP (*14*, *15*). The product of Cnx1G is subsequently transferred in a molybdate-dependent manner to the adjacent Cnx1E domain where MPT−AMP is hydrolyzed in the presence of Zn^{2+} or Mg^{2+} and Moco is released (*16*).

Although eukaryotic monopterin cofactor maturation by Cnx1 is well-studied, the mechanism for the synthesis of bispterin cofactors of the DMSOR type is less understood. As Cnx1G reconstitutes *Escherichia coli* MogA function (*17*) one can assume that a similar chemistry involving formation of MPT−AMP is performed in bacteria. In addition, the Cnx1E homologous MoeA protein has been demonstrated to function in Mo insertion (*18*), but the lack of MoeA reconstitution by Cnx1E indicates significant differences in the metal insertion mechanism between bacteria and eukaryotes (*19*). Furthermore, attachment of nucleotides is required to complete the synthesis of bispterin guanine Mo cofactors in *E. coli* (*20*). In *E. coli*, out of the 10 products of four operons (*moaABCDE*, *mobAB*, *moeAB*, and *mogA*) eight proteins were found to be essential for the biosynthesis of Moco. For two proteins, MoaB and MobB, a functional requirement in this pathway is unproven as none of the available nitrate reductase-deficient mutants were associated with their loci (*3*).

In contrast to that of Moco, synthesis of Wco has not been studied so far. However, it is likely that the basic mechanisms of Wco and Moco synthesis are similar as almost all genes that have an assigned function in the Moco biosynthetic pathway are also present in the genome of organisms that use tungsten in their metabolism. Main differences should occur in the metal insertion step as here a specific discrimination between Mo and W is required. For example, recent work on the assembly of the Mo-dependent nitrate reductase in *E. coli* showed that cofactor insertion into apo-nitrate reductase is lost in the presence of tungsten, indicating that a W-substituted nitrate reductase does not exist in *E. coli* (*21*). However, the molybdenum in *E. coli* trimethylamine *N*-oxide (TMAO) reductase could be replaced with tungsten resulting in an active form of the enzyme (*22*). TMAO reductase and nitrate reductase both contain a bis-MGD cofactor, and therefore, the type of cofactor is apparently not determining the metal specificity. The selective metal incorporation is also not strictly dependent on the transporter system as molybdate (ModA) and tungstate transporters (TupA and WtpA) are known to bind both oxoanions, be it with different affinities. For example, the recently identified tungstate transporter from *P. furiosus* selectively binds tungstate with a 1000-fold higher affinity over molybdate (*23*).

MogA and MoeA are known to be important for *E. coli* Mo insertion; however, in *P. furiosus* and other archaea only the MogA-homologous MoaB proteins are found. In addition, two different MoeA orthologs are present in these genomes. We have chosen the hyperthermophilic archaeon *P. furiosus*, which is strictly dependent on tungstate and grows optimally at 100 °C under anaerobic conditions (*24*), as a model organism to study Wco biosynthesis. Here we report that *P. furiosus* MoaB as well as *E. coli* MogA catalyze MPT adenylylation, a finding that demonstrates the universal existence of MPT−AMP in the biosynthesis of both tungsten as well as molybdenum cofactors.

EXPERIMENTAL PROCEDURES

Plasmids, Bacterial Strains. The following *E. coli* mutant strains were used: RK5206 (*mogA*) [RK4353 *chlG206::Mu cts mogA*] and RK4353 (*25*) that were cultured at 30 °C.

Cloning of P. furiosus and E. coli moaB and mogA Genes. The *moaB* genes, PF00372 (*P. furiosus*) and b0782 (*E. coli*), were amplified by PCR using *Pfx* polymerase (Invitrogen) and chromosomal DNA from *P. furiosus* or *E. coli* DH5α as a template, respectively. Extraction of the chromosomal DNA was performed with phenol/chloroform/isoamylalcohol. PCR products were treated with *Taq* polymerase (Amersham Bioscience) for 10 min at 72 °C to obtain single 3′adenine overhangs for subcloning into the pCR2.1-TOPO vector (Invitrogen). TOPO-constructs were transformed into competent *E. coli* TOP10 cells (Invitrogen), plasmids were isolated and after sequencing positive fragments were cloned into the *Nde1* and *BamH1* sites of the pET15b (Novagen), resulting in MoaB fusion proteins with an N-terminal his-tag. These constructs were transformed into competent *E. coli* BL21- CodonPlus-(DE3)-RIPL cells (Stratagene). *E. coli* mogA was PCR-cloned into the NdeI/XhoI sites of pET22b plasmid (Novagen) and transformed into BL21 (DE3) cells (Stratagene). Site-directed mutagenesis was performed by PCR on the expression plasmid pET15b-PfMoaB using the QuickChange site-directed mutagenesis kit (Stratagene).

Determination of Nitrate Reductase Activity in E. coli. The λDE3 lysogenization procedure (Novagen) was used to integrate the gene for T7 polymerase into the chromosome of the RK5206 *mogA*- strain. The resulting strain RK5206-(DE3) was transformed with the corresponding pET15b constructs containing PfMoaB variants or EcMoaB. The cells were cultured as described, and nitrate reductase activity was determined spectrophotometrically using reduced benzyl viologen as electron donor (*26*).

Protein Production and Purification of PfMoaB and Homologous E. coli Proteins. E. coli BL21(DE3) cells containing pET15b-PfMoaB or pET15b-EcMoaB were grown aerobically in Luria broth medium containing 100 μg/mL ampicillin. Protein synthesis was induced with a final concentration of 0.5 mM IPTG, when the absorbance of the culture reached 0.5 at 600 nm. Cells were induced for 5 h at 30 °C, harvested by centrifugation, washed with buffer A (20 mM Tris−HCl, pH 8.0, 10 mM imidazole, 500 mM NaCl, and 10% glycerol), and lysed in the same buffer (1 g of cells/5 mL of buffer) using a cell disruptor system (Constant systems). Cell-free extract was obtained by centrifugation for 20 min at 15 000*g* at 4 °C. In the case of the PfMoaB, the supernatant was heated for 30 min at 70 °C as a first purification step. Precipitated protein was removed by centrifugation, and the supernatant was applied to a Ni−sepharose 6 fast flow resin (GE healthcare) equilibrated with buffer A, washed with the same buffer, and eluted with buffer B (20 mM Tris−HCl, pH 8.0, 500 mM imidazole, 500 mM NaCl, and 10% glycerol). Protein-containing samples were dialyzed against buffer C (20 mM Tris, pH 8.0, 250 mM NaCl, and 10% glycerol), concentrated, and applied to a Superdex-200 HR27/60 column

equilibrated with buffer C. Fractions eluting under the main peak were pooled, concentrated (10 mg/mL), and stored at −80 °C. Overproduction of EcMogA was performed in Luria broth medium supplemented with 0.2 mM IPTG at 37 °C under aerobic conditions. Protein extracts were prepared as described above using 20 mM Tris−HCl, pH 7.6, 500 mM NaCl, 5 mM imidazole buffer and applied to a Ni^{2+} affinity column (HiTrap, GE Healthcare) equilibrated with the same buffer. After washing the column, the EcMogA was eluted with 200 mM imidazole and protein-containing fractions were pooled, dialyzed against 20 mM Tris−HCl, pH 7.6, 0.1 M NaCl buffer, frozen in liquid nitrogen, and stored at −80 °C until used.

In Vitro Synthesis and Analysis of MPT and MPT−AMP. MPT was synthesized in vitro using purified cyclic pyranopterin monophosphate (cPMP) (*27*), as well as purified *E. coli* MPT synthase (*28*) or *E. coli* MoaE and *E. coli* thiocarboxylated MoaD that were purified and assembled into active MPT synthase as described before (*28*). Standard in vitro MPT synthesis was performed in MPT buffer (100 mM Tris, pH 7.2) containing 1000 pmol cPMP, 250 pmol MoaB, 20 pmol MoaE and 100 pmol MoaD in an assay volume of 140 μL per point of measurement and incubated at room temperature for 30 min to saturate MPT synthesis. Subsequently, the mixture was incubated for 2 min at the temperature required for the adenylylation, which was 65 °C under standard conditions for PfMoaB. The adenylylation reaction was initiated upon addition of nucleotide and divalent cations. At different time points, samples (140 μL) were taken directly from the reaction mixture and the reaction was stopped by the addition of 17.5 μL of 1% I_2, 2% KI, 1 M HCl. MPT and MPT−AMP were determined by HPLC formA (i.e., MPT iodine oxidized product) analysis as described (*15*) with the variation that 200 μL Q-sepharose columns (GE healthcare) were used to purify formA and formA−AMP prior HPLC analysis.

RESULTS

Expression and Purification of MoaB Variants. PfMoaB shows high homology at the primary sequence level to EcMoaB, MogA, and Cnx1G (Figure 1A). Superimposition of Cnx1G−MPT−AMP complex structure (*14*) with the available crystal structures of *E. coli* MogA (*29*) and *E. coli* MoaB (*30*, *31*) demonstrates a high degree of structural conservation surrounding the hypothetical active sites of all three proteins (Figure 1B). The sequence alignment of MoaB- and MogA-homologous proteins confirms the conservation of residues that have been shown to be important for substrate (MPT) binding and catalysis (adenylyl transfer) in Cnx1G. Therefore, we have replaced three hypothetical active residues in PfMoaB in order to generate variants that are proposed to be affected in their MPT-binding site (S112A), nucleotide-binding site (D32A), and catalysis (D56A) (Figure 1A, black arrows). Adjacent to D56, D57 seems to be less conserved (Figure 1A) as some proteins including *E. coli* MogA contain a glutamate. In order to generate a protein more similar to the active site of *E. coli* MogA we also generated the PfMoaB variant D57E. Wild-type PfMoaB, its variants, and EcMoaB and MogA were recombinantly expressed in *E. coli* as N-terminally His-tagged proteins and purified to homogeneity (see Experimental Procedures). For all variants average yields of 10−15 mg/L culture were obtained.

Reconstitution of E. coli Moco Biosynthesis. In view of the conservation at the primary sequence level between PfMoaB and MogA proteins, we investigated whether an *E. coli mogA* (RK5206) mutant could be complemented by PfMoaB, EcMoaB, or by positive control *E. coli* MogA. Production of wild-type PfMoaB in *mogA*-deficient cells restored Moco synthesis, which was monitored by the reconstitution of nitrate reductase activity (Figure 1C). In contrast, EcMoaB did not show any complementation, whereas EcMogA restored activity to the level of the wild type. This observation showed that (i) PfMoaB can replace MogA in bacterial Moco biosynthesis and that (ii) the thermophilic PfMoaB is also able to function at 30 °C, which was the growth temperature of the *E. coli mogA* mutant. The variant D56A expected to be impaired in catalysis (*17*), showed a complete loss of function, as nitrate reductase activity was similar to cells transformed with control plasmid (Figure 1C). Variants with changes in the hypothetical substrate-binding site for MPT (S112A) and the nucleotide-binding site (D32A) retained their activity or showed only a partially reduced activity, respectively. The PfMoaB D57E variant mimicking the active site structure of MogA also restored nitrate reductase activity completely.

MPT Binding. Successful reconstitution of Moco synthesis in *E. coli* demonstrated that PfMoaB participates in a similar reaction as catalyzed by MogA in bacterial Moco biosynthesis. Therefore, we investigated the ability of PfMoaB to bind MPT, the starting molecule for the adenylyl transfer reaction.

First, size exclusion chromatography of PfMoaB was performed. Wild-type PfMoaB (Figure 2A) as well as all variants (data not shown) eluted at a molecular weight of ca. 120 kDa. As monomeric PfMoaB has a theoretical mass of 20.7 kDa we conclude that it forms hexamers as the main oligomeric form. A smaller peak eluted before the main PfMoaB peak, which was found to also contain PfMoaB protein that formed higher ordered oligomers (ca. 300 kDa). No significant absorption at 375 nm was observed, which was consistent with MPT determinations (data not shown) that showed no copurification of MPT with PfMoaB upon overproduction in *E. coli*.

Next, MPT was synthesized in vitro using purified MPT synthase (*28*) and excess purified cPMP (*27*) and coincubated with PfMoaB. We used 2 nmol of MPT synthase and 10 nmol of cPMP to synthesize MPT, which was subsequently coincubated under anaerobic conditions with 30 nmol of PfMoaB. The reaction mixture was separated by size exclusion chromatography, and no change in the oligomeric state of PfMoaB was detectable (Figure 2B). However, upon coincubation with the MPT synthase reaction a strong absorption at 375 nm was detectable under the hexameric as well as under the high molecular weight peak of PfMoaB. The hexameric PfMoaB peak was collected and concentrated to 314 μM. HPLC FormA analysis revealed that 11 μM MPT (1650 pmol) was bound to the PfMoaB hexamer, whereas only trace amounts of MPT retained on MPT synthase (data not shown). Substoichiometric saturation with MPT was due to the excess of PfMoaB.

P. furiosus MoaB Catalyzes MPT Adenylylation. Having shown MPT binding to PfMoaB we investigated its ability

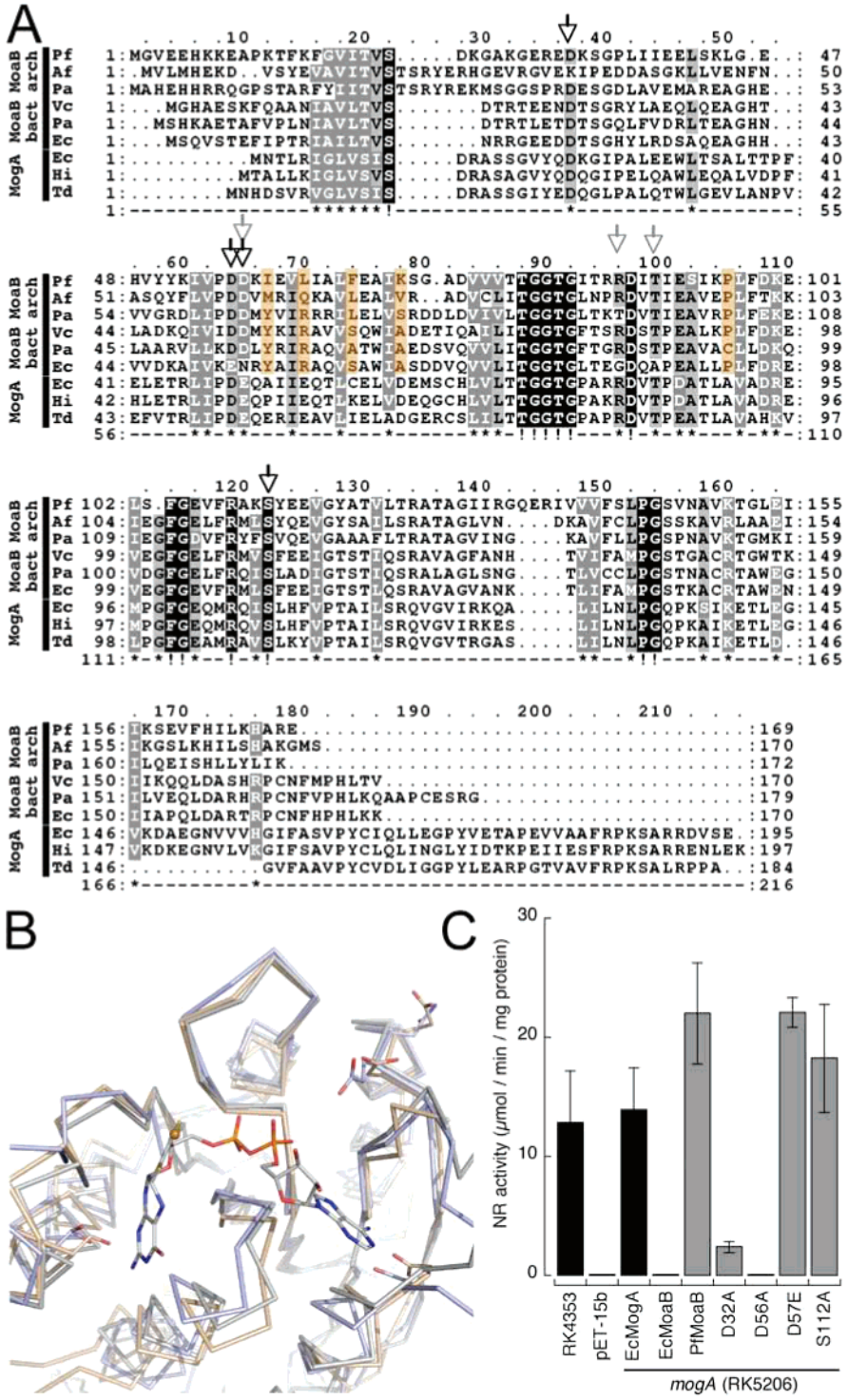

FIGURE 1: Sequence and structural comparison of MoaB, MogA, and Cnx1G. (A) Multiple sequence alignment of *P. furiosus* MoaB (PF0372), *Archaeoglobus fulgidus* MoaB (AF0265), *Pyrobaculum aerophilum* MoaB (PAE0969), *Vibrio cholerae* MoaB (VC1025), *Pseudomonas aeruginosa* MoaB (PA3029), *E. coli* MoaB (b0782), *E. coli* MogA (b0009), *Haemophilus influenzae* MogA (NTHI0454), and *Thiobacillus denitrificans* MogA (Tbd2143) listed in the order of appearance. The alignment was generated with ClustalW, consensus sequence calculation and shadings were performed using a threshold of 75% for conserved residues. Completely conserved residues show an exclamation mark (!) in the consensus line and are printed in white letters (shaded dark). Highly conserved residues (white letters) and low conserved residues (black letters) are shaded in gray. Residues subjected to mutagenesis are marked with a black arrow, whereas residue positions that are specifically altered in EcMoaB are highlighted with a gray arrow. Residues forming contacts in the EcMoaB trimer are overlaid with an orange box. (B) Structural comparison of Cnx1G (S583A variant, shown in gray) with bound MPT−AMP (1UUY) and *E. coli* proteins MogA (1DI6, blue) and MoaB (1MKZ, orange). Corresponding residues that were mutated in PfMoaB are highlighted in the structure of EcMogA as well as EcMoaB. The figure was generated with COOT (www.ysbl.york.ac.uk/~emsley/coot) and rendered with POVRAY (www.povray.org). (C) Functional reconstitution of nitrate reductase activity in *E. coli mogA* mutants upon production of *E. coli* MogA and MoaB as well as wild-type and mutant PfMoaB variants. The *E. coli* RK4353 strain was used as positive control, and RK5206 (*mogA*) strain transformed with the empty vector was taken as negative control.

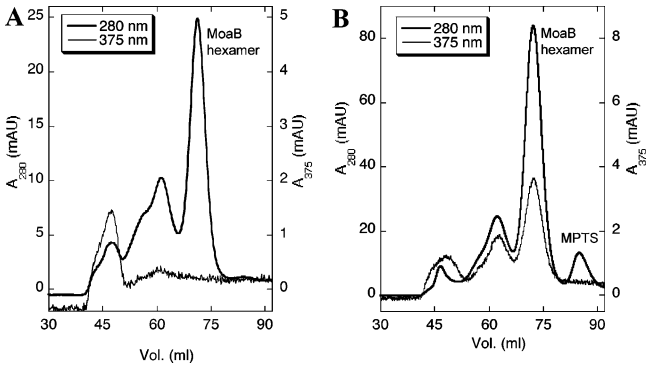

FIGURE 2: Transfer of MPT to purified PfMoaB. (A) Size exclusion chromatogram of purified PfMoaB (10 nmol) indicating its hexameric structure. (B) Size exclusion chromatogram of PfMoaB (30 nmol) and MPT synthase (2 nmol) showing efficient transfer of MPT from MPT synthase to PfMoaB.

to catalyze a similar nucleotidyl transfer reaction as previously described for plant Cnx1G (*15*). For all subsequent functional studies of PfMoaB we used purified *E. coli* MoaE protein (large subunit of MPT synthase) and thiocarboxylated MoaD protein (small subunit of MPT synthase) that were in vitro assembled to form fully active MPT synthase converting cPMP into MPT in vitro (*28*). MPT synthesis was performed in the presence of excess cPMP (2000 pmol) and 250 pmol of PfMoaB for 60 min to ensure quantitative MPT synthesis and transfer to PfMoaB.

First, we investigated the ability of PfMoaB to catalyze MPT adenylylation under similar conditions as previously used for plant Cnx1G (*15*). The reaction was initiated with 1 mM ATP and 10 mM $MgCl_2$. MPT−AMP formation and MPT consumption were monitored by HPLC formA and formA−AMP analysis (Figure 3). At room temperature we found an almost complete conversion of MPT (50 pmol) into MPT−AMP (70 pmol) within 120 min (Figure 3A). The increase in MPT−AMP in comparison to the starting amount of MPT is due to ongoing MPT synthesis by the MPT synthase. The velocity of MPT adenylylation at room temperature was comparable to previous results with Cnx1G, where most of the MPT−AMP was synthesized within the first 60 min of the reaction (in the absence of inorganic pyrophosphatase) (*15*). Prolonged incubation (above 180 min) caused progressive degradation of MPT−AMP (Figure 3A).

As PfMoaB derives from a hyperthermophilic organism, we also studied the temperature dependence of MPT adenylylation. It is important to note that Moco and MPT are extremely unstable even when they are bound to different (eukaryotic) Mo-dependent enzymes: they can be rapidly released and oxidized by heat denaturation (*13*). The initial MPT synthesis reaction including binding of MPT to PfMoaB was performed at room temperature. Subsequently, the reaction mixtures were heated to the indicated temperatures and incubated for 2 min before adenylylation was started by the addition of Mg−ATP. A strong acceleration in MPT−AMP synthesis was observed with increasing temperatures with a maximum at 80 °C (Figure 3B). In the range of 50−80 °C quantitative conversion of MPT into MPT−AMP was indicated by saturation of MPT−AMP formation and depletion of MPT (data not shown), while at 25 °C the reaction was not completed within the investigated time frame. Additionally, with prolonged reaction time

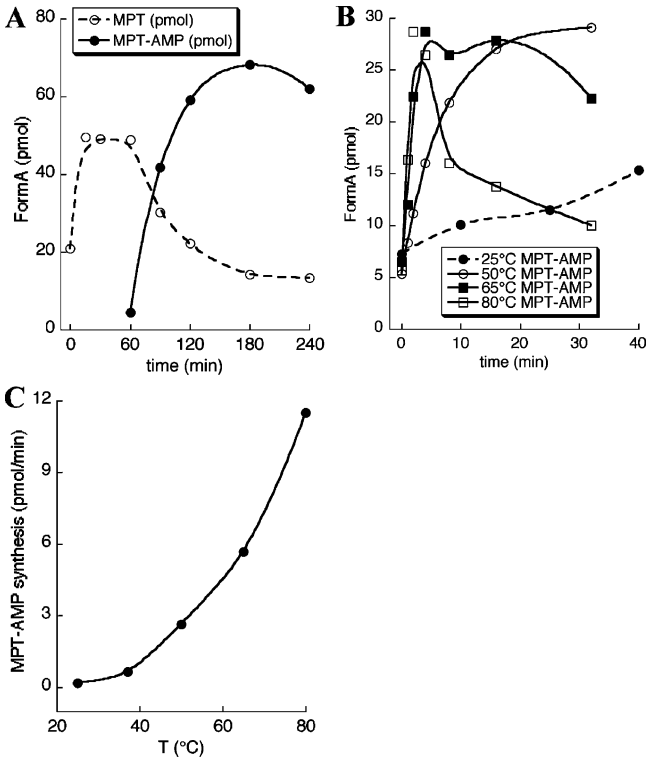

FIGURE 3: Adenylylation of MPT by PfMoaB. MPT was in vitro synthesized by using purified *E. coli* MoaE and thiocarboxylated MoaD proteins and purified cPMP. After 60 min MPT synthesis adenylylation was started by adding 1 mM ATP and 10 mM $MgCl_2$. MPT and MPT−AMP were determined by HPLC formA and formA−AMP analysis. (A) MPT adenylylation at room temperature by monitoring MPT depletion and MPT−AMP formation. (B) Temperature-dependent MPT adenylylation kinetics (MPT−AMP synthesis). (C) Initial reaction velocities at different temperatures.

MPT−AMP levels rapidly decreased at higher temperature, probably due to degradation of the compound, or degradation of PfMoaB, or both. Subsequent experiments were performed at 65 °C because PfMoaB remained stable at that temperature and the velocity of the reaction enables accurate kinetic determinations. Finally, we analyzed MPT−AMP formation (taken from the initial velocity) as a function of reaction temperature (Figure 3C), which followed a typical activity profile of a thermostable enzyme. A maximal synthesis of 12 pmol of MPT−AMP per min was found at 80 °C, which is more than 20 times higher than the corresponding velocity of PfMoaB at room temperature.

Next we determined the kinetic parameters of PfMoaB using MPT and Mg−ATP as substrates (Figure 4, parts A and B). We recorded MPT adenylylation velocities for four different ATP concentrations (30−1000 μM) resulting in a K_M value of 220 μM ATP and a maximal velocity of 18.6 pmol MPT−AMP/min. In comparison to Cnx1G (*15*), the K_M and v_{max} are, respectively, 4 and 20 times higher for PfMoaB.

Substrate Specificity of PfMoaB. In view of the unusual growth conditions of *P. furiosus*, we tested alternative substrates and cosubstrates that might be used for nucleotidylylation of MPT. For example, some hyperthermophilic enzymes are known to use ADP as substrate in contrast to their mesophilic homologues that operate with ATP, and this is thought to be related to a higher thermostability of ADP (*32*). However, no other nucleotide was found to exhibit

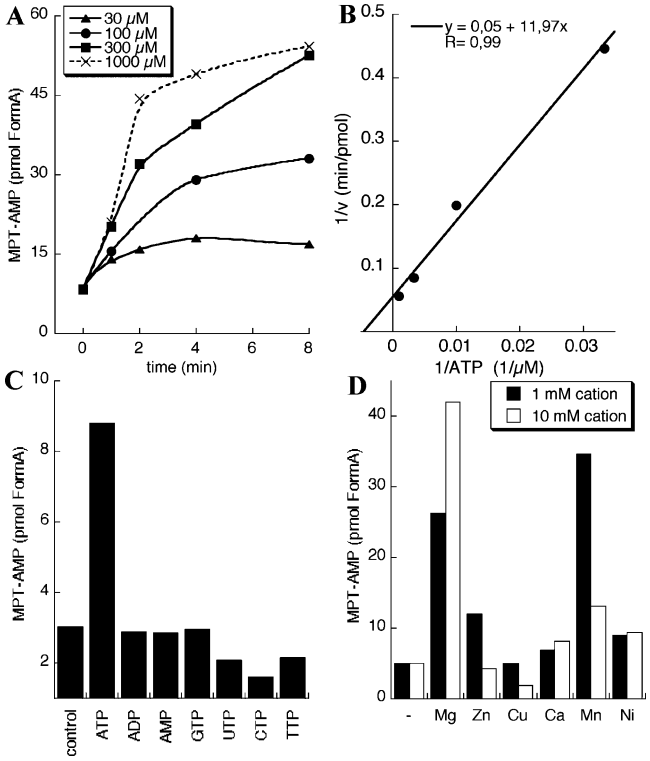

FIGURE 4: Nucleotide- and metal-dependent PfMoaB activity. (A) ATP-dependent adenylylation of MPT at 65 °C and (B) reciprocal plot of the obtained reaction velocities. (C) PfMoaB-catalyzed formation of MPT−nucleotidylylates with different nucleotides (1 mM) in the presence of 10 mM $MgCl_2$ at 65 °C. (D) Cation-dependent adenylylation of MPT in the presence of 1 mM ATP at 65 °C at 1 and 10 mM of the respective cation.

significant activity in the formation of nucleotidylylated MPT (Figure 4C). Apparently, adenylyl transfer to MPT represents an evolutionarily conserved mechanism important for the maturation of both molybdenum and tungsten cofactors. Regarding the specificity of PfMoaB for different divalent cations as cosubstrates, Mg^{2+} and Mn^{2+} exhibited comparable activity with Mn^{2+} being even more active at lower concentrations (Figure 4D).

Characterization of PfMoaB Variants. Next, we investigated the functional properties of the PfMoaB variants previously studied by functional reconstitution of *E. coli mogA* mutants. Variants with no (D56A) or strongly reduced (D32A) activity in *E. coli* were also inactive in MPT−AMP synthesis (Figure 5A). However, D57E, which was expected to be as active as wild-type PfMoaB (Figure 1C), showed somewhat less activity under the experimental conditions, whereas variant S112A with hypothetically impaired MPT binding was even more active than wild-type PfMoaB (Figure 5A) indicating that this residues does not contribute significantly to MPT binding in PfMoaB.

Comparison of PfMoaB to Its Bacterial Homologues E. coli MogA and MoaB. The fact that PfMoaB as well as Cnx1G reconstitutes *E. coli mogA* mutants strongly suggests that MogA catalyzes the same reaction as Cnx1G and PfMoaB. Therefore, we expressed and purified *E. coli* MogA and subjected it to standard adenylyl transfer experiments (Figure 5B). MogA was able to catalyze MPT adenylylation even more efficiently than PfMoaB at 37 °C. These results confirm unequivocally that all protein members of the MoaB/MogA/Cnx1G family catalyze the same MPT activation reaction essential for metal transfer into different pterin cofactors.

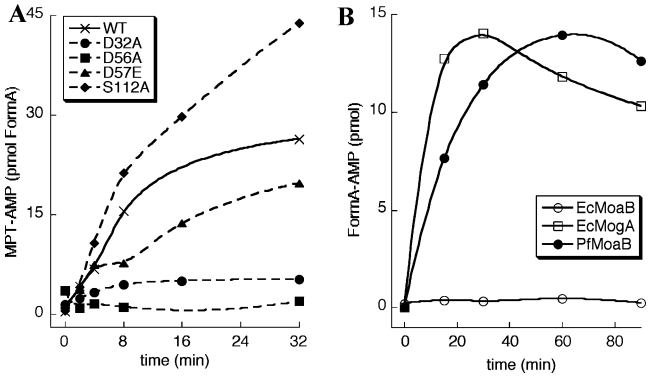

FIGURE 5: Functional characterization of PfMoaB variants and *E. coli* MogA and MoaB. (A) MPT adenylylation by PfMoaB variants under standard conditions with 1 mM ATP and 10 mM $MgCl_2$ at 65 °C. (B) MPT adenylylation by PfMoaB, *E. coli* MogA, and *E. coli* MoaB under standard conditions at 37 °C.

A final experiment addressed the functional properties of *E. coli* MoaB (EcMoaB) in vitro. The fact that *mogA* mutants are Moco deficient suggests that EcMoaB is unable to replace MogA function in *E. coli*, which was further strengthened by the inability of EcMoaB to complement *mogA* mutants even after overexpression (Figure 1C). In order to prove this proposal we purified EcMoaB as His-tagged protein and subjected it to MPT−AMP synthesis experiments (Figure 5B). The results clearly demonstrated that *E. coli* MoaB is not able to perform an adenylyl transferase reaction (Figure 5B) although it is able to bind MPT in vitro (data not shown). Our results show for the first time that the *E. coli* representative of the family of MoaB proteins has no catalytic function in Mo cofactor biosynthesis although it is expressed in the *moa* operon encoding four other proteins involved in bacterial Moco biosynthesis.

DISCUSSION

Mo- and W-containing enzymes share the same pterin-based scaffold chelating the reactive metals to ene-dithiolate groups. The basic physicochemical properties of these metals are very similar, and it is therefore likely that a common, probably highly conserved, mechanism has evolved to transform both transition metals into biocatalysts (*33*). At the same time very restrictive reactions should enable a clear discrimination between these related metals as they are both bioavailable and known to often represent antagonists for each other. Although Mo-containing enzymes are found in all kingdoms of life, W-dependent enzymes are restricted to prokaryotes and are mostly found in archaea (*5*).

Analyses of archaeal genomes identified a complete set of genes homologous to genes encoding proteins involved in the biosynthesis of Moco. Therefore, a general conservation in the biosynthesis of the MPT pterin backbone has been proposed (*33*). However, little is known about how organisms discriminate between molybdenum and tungsten. Recent studies regarding tungstate uptake in *P. furiosus* showed high substrate specificity of WtpA (*23*), the periplasmic oxoanion-binding protein of the high-affinity ABC-type tungstate uptake system for which recently a crystal structure has been determined from a related organism (*34*). In order to uncover common and metal-specific processes in Moco and Wco biosynthesis we investigated the function of *P. furiosus* MoaB, a protein of hitherto unknown function but with clear homology to the Cnx1G domain (*35*). As Cnx1G was the first and so far only protein for which a novel MPT

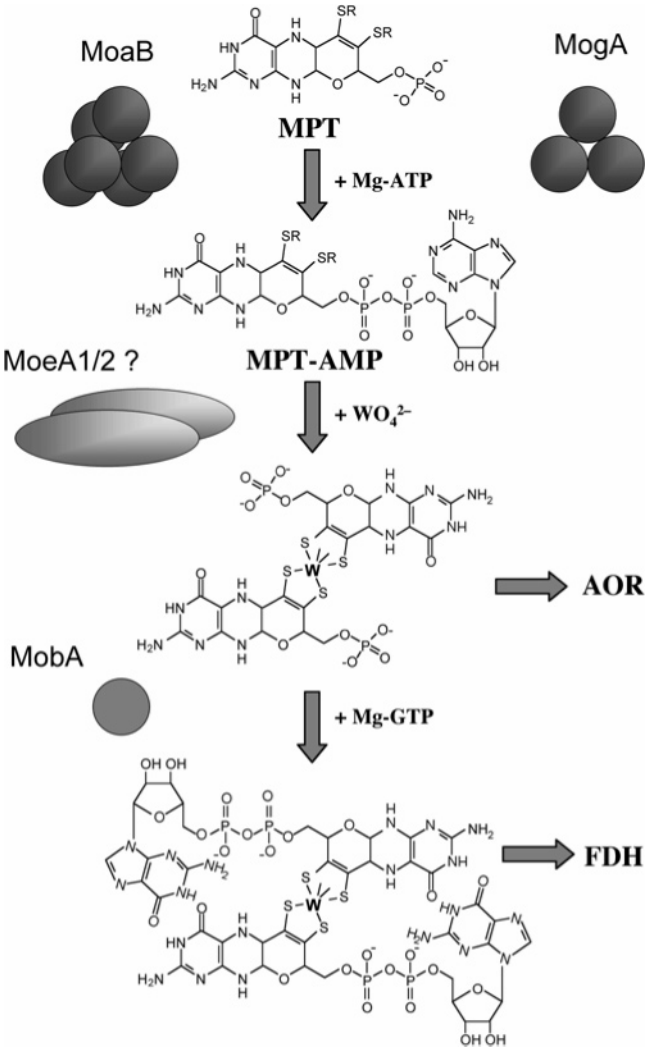

FIGURE 6: Model for the last steps in tungsten cofactor biosynthesis of *P. furiosus*. Shown are the steps following MPT synthesis in *P. furiosus* leading to the formation of bispterin W cofactor *as* found in enzymes of the aldehyde oxidoreductase (AOR) family and bispterin W-containing guanine dinucleotide cofactor found in formate dehydrogenase (FDH). First, MPT is adenylylated by the action of the hexameric MoaB, a function which is identical to the trimeric MogA protein found in *E. coli*. Next, the metal is inserted by MoeA1 or MoeA2 or both. Finally, guanylylation has to be catalyzed by the MobA protein. In MPT and MPT−AMP both dithiolene ligands are indicated by an R as the ligand is not known so far.

adenylylation function has been described (*14*, *15*) it was crucial to know if this reaction is common for Moco biosynthesis and if similar or even identical mechanisms are important for Wco biosynthesis.

We have shown here that *P. furiosus* MoaB and *E. coli* MogA catalyze the same adenylylation reaction as plant Cnx1G in order to activate the MPT for metal insertion. Therefore, MPT−AMP synthesis is not only crucial for eukaryotic Moco biosynthesis, but it represents a common and well-conserved reaction intermediate essential for the synthesis of Mo and W cofactor in all kingdoms of life. As a result, MogA and MoaB proteins can be classified as pterin adenylyl transferases similar to Cnx1G (Figure 6).

Interestingly, *E. coli* MoaB was found to be inactive in MPT adenylylation. When comparing EcMoaB to different MogA and MoaB proteins a few but very specific changes of otherwise conserved residues (N53, G84, A87) are observed (Figure 1A, gray arrows). Similar to *E. coli* MoaB such changes are also found in other orthologs that are coexpressed with a (hypothetically) active MogA protein in the same organism such as in *Salmonella enterica choleraesuis*, *Klebsiella pneumoniae*, or *Erwinia carotovora atroseptica*.

In conclusion, EcMoaB is not directly involved in *E. coli* Moco synthesis, but it might have other yet unknown functions related to this pathway. For example, the ability to bind MPT (data not shown) might point to a regulatory role in sensing the pterin and/or Mo cofactor status of the cell. A key regulatory site in bacterial Moco synthesis is the *E. coli moa* operon, which is controlled by molybdate as well as by levels of active cofactor (*36*).

Genomic inspections showed that the functionally inactive sequence of *E. coli* MoaB forms the exception and that most other MoaBs are expected to be active adenylyl transferases like PfMoaB. These adenylyl transferases are most abundant among archaea, as no archaeal genome sequenced so far contains a gene for a MogA homologue. As *E. coli* MogA and other homologous proteins such as plant (*19*) and *Chlamydomonas* Cnx1G (*37*) as well as gephyrin G domain form trimers in solution (*38*), one can conclude that these proteins represent a unique family of trimeric adenylyl transferases. Regarding MoaB, structural information is limiting, as only EcMoaB has been determined so far. Therefore, PfMoaB represents the second characterized hexameric MoaB protein and more studies are needed to confirm that MoaB proteins are in general hexameric. However, inspection of the trimer interface in EcMoaB reveals that at least three (Tyr55, Arg58, Pro92) out of the five residues that mediate contacts between the two MoaB trimers are conserved in MoaB-homologous proteins (Figure 1A). It is even more important that in MogA-like proteins these residues are replaced by residues with either opposite charge or different character (EcMogA Ala52, Glu55, Ala90). The nonexistence of archaeal trimeric adenylyl transferases combined with the abundance of MoaB proteins in archaeal (hyper)thermophiles leads to the hypothesis that thermostability of PfMoaB relies in part on its hexameric structure. As the hexamer interface does not interfere with the active site of MoaB proteins, future experiments should allow detailed structure−function studies to uncover the molecular basis of thermal stability. Furthermore, the trimeric and hexameric adenylyl transferases might contribute differently downstream in the pathway, such as in bispterin formation or metal insertion (Figure 6).

On the basis of our results MPT−AMP represents the last common intermediate of Moco and Wco biosynthesis, and selective metal incorporation should therefore rely on the oxyanion-dependent hydrolysis of MPT−AMP, as described for plant Cnx1E domain (*16*) which is very specific for molybdate. Therefore, Cnx1E-homologous MoeA proteins from bacteria or archaea should also hydrolyze MPT−AMP in a molybdate- and/or tungstate-dependent manner. The fact that eukaryotic Cnx1E cannot replace the function of *E. coli* MoeA (*19*) suggests different mechanisms in metal insertion, possibly due to the formation of bis-metal−pterin cofactors in prokaryotes (including W cofactors). The finding that in *P. furiosus* and in many other archaeal genomes two different MoeA (PfMoeA1 and PfMoeA2) proteins are expressed might either point to metal selectivity or to the formation of the two different tungsten cofactors known so far (Figure 6). Uncovering these mechanisms and understanding how

they differ between Moco and Wco synthesis are main challenges for the future.

ACKNOWLEDGMENT

We thank Simona Cerrone and Sarah Nicklas (University of Cologne) for technical assistance.

REFERENCES

1. Hille, R. (1996) The mononuclear molybdenum enzymes, *Chem. Rev. 96*, 2757−2816.
2. Kletzin, A., and Adams, M. W. (1996) Tungsten in biological systems, *FEMS Microbiol. Rev. 18*, 5−63.
3. Rajagopalan, K. V., and Johnson, J. L. (1992) The pterin molybdenum cofactors, *J. Biol. Chem. 267*, 10199−10202.
4. Schwarz, G. (2005) Molybdenum cofactor biosynthesis and deficiency, *Cell. Mol. Life Sci. 62*, 2792−2810.
5. Hille, R. (2002) Molybdenum and tungsten in biology, *Trends Biochem. Sci. 27*, 360−367.
6. Hille, R. (2005) Molybdenum-containing hydroxylases, *Arch. Biochem. Biophys. 433*, 107−116.
7. Robb, F. T., Maeder, D. L., Brown, J. R., DiRuggiero, J., Stump, M. D., Yeh, R. K., Weiss, R. B., and Dunn, D. M. (2001) Genomic sequence of hyperthermophile, *Pyrococcus furiosus*: implications for physiology and enzymology, *Methods Enzymol. 330*, 134−157.
8. Mukund, S., and Adams, M. W. (1991) The novel tungsten−iron−sulfur protein of the hyperthermophilic archaebacterium, *Pyrococcus furiosus*, is an aldehyde ferredoxin oxidoreductase. Evidence for its participation in a unique glycolytic pathway, *J. Biol. Chem. 266*, 14208−14216.
9. Roy, R., Mukund, S., Schut, G. J., Dunn, D. M., Weiss, R., and Adams, M. W. W. (1999) Purification and molecular characterization of the tungsten-containing formaldehyde ferredoxin oxidoreductase from the hyperthermophilic archaeon *Pyrococcus furiosus*: the third of a putative five-member tungstoenzyme family, *J. Bacteriol. 181*, 1171−1180.
10. Mukund, S., and Adams, M. W. (1995) Glyceraldehyde-3-phosphate ferredoxin oxidoreductase, a novel tungsten-containing enzyme with a potential glycolytic role in the hyperthermophilic archaeon *Pyrococcus furiosus*, *J. Biol. Chem. 270*, 8389−8392.
11. Roy, R., and Adams, M. W. W. (2002) Tungsten-dependent aldehyde oxidoreductase: A new family of enzymes containing the pterin cofactor, *Met. Ions Biol. Syst. 39*, 673−697.
12. Bevers, L. E., Bol, E., Hagedoorn, P.-L., and Hagen, W. R. (2005) WOR5, a novel tungsten-containing aldehyde oxidoreductase from *Pyrococcus furiosus* with a broad substrate specificity, *J. Bacteriol. 187*, 7056−7061.
13. Schwarz, G., Boxer, D. H., and Mendel, R. R. (1997) Molybdenum cofactor biosynthesis. The plant protein Cnx1 binds molybdopterin with high affinity, *J. Biol. Chem. 272*, 26811−26814.
14. Kuper, J., Llamas, A., Hecht, H. J., Mendel, R. R., and Schwarz, G. (2004) Structure of molybdopterin-bound Cnx1G domain links molybdenum and copper metabolism, *Nature 430*, 806−806.
15. Llamas, A., Mendel, R. R., and Schwarz, G. (2004) Synthesis of adenylated molybdopterin: an essential step for molybdenum insertion, *J. Biol. Chem. 279*, 55241−55246.
16. Llamas, A., Otte, T., Multhaup, G., Mendel, R. R., and Schwarz, G. (2006) The mechanism of nucleotide-assisted molybdenum insertion into molybdopterin. A novel route toward metal cofactor assembly, *J. Biol. Chem. 281*, 18343−18350.
17. Kuper, J., Palmer, T., Mendel, R. R., and Schwarz, G. (2000) Mutations in the molybdenum cofactor biosynthetic protein Cnx1G from *Arabidopsis thaliana* define functions for molybdopterin bind, Mo-insertion and molybdenum cofactor stabilization, *Proc. Natl. Acad. Sci. U.S.A. 97*, 6475−6480.
18. Nichols, J. D., and Rajagopalan, K. V. (2005) In vitro molybdenum ligation to molybdopterin using purified components, *J. Biol. Chem. 280*, 7817−7822.
19. Schwarz, G., Schulze, J., Bittner, F., Eilers, T., Kuper, J., Bollmann, G., Nerlich, A., Brinkmann, H., and Mendel, R. R. (2000) The molybdenum cofactor biosynthetic protein Cnx1 complements molybdate-repairable mutants, transfers molybdenum to the metal binding pterin, and is associated with the cytoskeleton, *Plant Cell 12*, 2455−2472.
20. Temple, C. A., and Rajagopalan, K. V. (2000) Mechanism of assembly of the bis(molybdopterin guanine dinucleotide)molybdenum cofactor in *Rhodobacter sphaeroides* dimethyl sulfoxide reductase, *J. Biol. Chem. 275*, 40202−40210.
21. Vergnes, A., Pommier, J., Toci, R., Blasco, F., Giordano, G., and Magalon, A. (2006) NarJ chaperone binds on two distinct sites of the aponitrate reductase of *Escherichia coli* to coordinate molybdenum cofactor insertion and assembly, *J. Biol. Chem. 281*, 2170−2176.
22. Buc, J., Santini, C. L., Giordani, R., Czjzek, M., Wu, L. F., and Giordano, G. (1999) Enzymatic and physiological properties of the tungsten-substituted molybdenum TMAO reductase from *Escherichia coli*, *Mol. Microbiol. 32*, 159−168.
23. Bevers, L. E., Hagedoorn, P. L., Krijger, G. C., and Hagen, W. R. (2006) Tungsten transport protein A (WtpA) in *Pyrococcus furiosus*: the first member of a new class of tungstate and molybdate transporters, *J. Bacteriol. 188*, 6498−6505.
24. Fiala, G., and Stetter, K. O. (1986) *Pyrococcus furiosus* sp. nov. represents a novel genus of marine heterotrophic archaebacteria growing optimally at 100 DegC, *Arch. Microbiol. 145*, 56−61.
25. Stewart, V., and MacGregor, C. H. (1982) Nitrate reductase in *Escherichia coli* K-12: involvement of chlC, chlE, and chlG loci, *J. Bacteriol. 151*, 788−799.
26. Jones, R. W., and Garland, P. B. (1977) Sites and specificity of the reaction of bipyridylium compounds with anaerobic respiratory enzymes of *Escherichia coli*. Effects of permeability barriers imposed by the cytoplasmic membrane, *Biochem. J. 164*, 199−211.
27. Santamaria-Araujo, J. A., Fischer, B., Otte, T., Nimtz, M., Mendel, R. R., Wray, V., and Schwarz, G. (2004) The tetrahydropyranopterin structure of the sulfur-free and metal-free molybdenum cofactor precursor, *J. Biol. Chem. 279*, 15994−15999.
28. Gutzke, G., Fischer, B., Mendel, R. R., and Schwarz, G. (2001) Thiocarboxylation of molybdopterin synthase provides evidence for the mechanism of dithiolene formation in metal-binding pterins, *J. Biol. Chem. 276*, 36268−36274.
29. Liu, M. T., Wuebbens, M. M., Rajagopalan, K. V., and Schindelin, H. (2000) Crystal structure of the gephyrin-related molybdenum cofactor biosynthesis protein MogA from *Escherichia coli*, *J. Biol. Chem. 275*, 1814−1822.
30. Sanishvili, R., Beasley, S., Skarina, T., Glesne, D., Joachimiak, A., Edwards, A., and Savchenko, A. (2004) The crystal structure of *Escherichia coli* MoaB suggests a probable role in molybdenum cofactor synthesis, *J. Biol. Chem. 279*, 42139−42146.
31. Bader, G., Gomez-Ortiz, M., Haussmann, C., Bacher, A., Huber, R., and Fischer, M. (2004) Structure of the molybdenum-cofactor biosynthesis protein MoaB of *Escherichia coli*, *Acta Crystallogr., Sect. D: Biol. Crystallogr. 60*, 1068−1075.
32. Ito, S., Fushinobu, S., Yoshioka, I., Koga, S., Matsuzawa, H., and Wakagi, T. (2001) Structural basis for the ADP-specificity of a novel glucokinase from a hyperthermophilic archaeon, *Structure 9*, 205−214.
33. Schwarz, G., Hagedoorn, P. L., and Fischer, K. (2007) Molybdate and Tungstate: Uptake, Homeostasis, Cofactors, and Enzymes, in *Molecular Microbiology of Heavy Metals*, *Microbiology Monographs* (Nies, D., and Silver, S., Eds.) Springer, Berlin-Heidelberg.
34. Hollenstein, K., Frei, D. C., and Locher, K. P. (2007) Structure of an ABC transporter in complex with its binding protein, *Nature 446*, 213−216.
35. Stallmeyer, B., Nerlich, A., Schiemann, J., Brinkmann, H., and Mendel, R. R. (1995) Molybdenum co-factor biosynthesis: the *Arabidopsis thaliana* cDNA cnx1 encodes a multifunctional two-domain protein homologous to a mammalian neuroprotein, the insect protein cinnamon and three *Escherichia coli* proteins, *Plant J. 8*, 751−762.
36. Anderson, L. A., McNairn, E., Lubke, T., Pau, R. N., and Boxer, D. H. (2000) ModE-dependent molybdate regulation of the molybdenum cofactor operon moa in *Escherichia coli*, *J. Bacteriol. 182*, 7035−7043.
37. Llamas, A., Tejada-Jimenez, M., Gonzalez-Ballester, D., Higuera, J. J., Schwarz, G., Galvan, A., and Fernandez, E. (2007) *Chlamydomonas reinhardtii* CNX1E reconstitutes molybdenum cofactor biosynthesis in *Escherichia coli* mutants, *Eukaryotic Cell 6*, 1063−1067.
38. Schwarz, G., Schrader, N., Mendel, R. R., Hecht, H. J., and Schindelin, H. (2001) Crystal structures of human gephyrin and plant Cnx1 G domains: comparative analysis and functional implications, *J. Mol. Biol. 312*, 405−418.

BI7020487